Fermi National Accelerator Laboratory

FERMILAB-Conf-94/276-E

Physics at the Fermilab Collider

Melvyn J. Shochet

Enrico Fermi Institute and Department of Physics
5640 S. Ellis Ave. Chicago, IL. 60637

September 1994

Published Proceedings *Eighth Meeting of the Division of Particles and Fields of the American Physical Society (DPF'94), University of New Mexico*, Albuquerque, NM, August 2-6, 1994

Disclaimer

CDF/PUB/CDF/PUBLIC/2786
FERMILAB-CONF-94/276-E

PHYSICS AT THE FERMILAB COLLIDER

MELVYN J. SHOCHET
Enrico Fermi Institute and Department of Physics
University of Chicago, 5640 S. Ellis Ave., Chicago,
Illinois 60637, USA

ABSTRACT

The CDF and D0 experiments at the Fermilab Tevatron Collider have produced many results from the search for the top quark, the study of both the electroweak and strong interactions, the production and decay of b quarks, and the search for new high mass objects. A sample of recently obtained results are presented.

1. Introduction

The Fermilab Tevatron Collider provides $\bar{p}p$ collisions at a center of mass energy of 1.8 TeV. During the 1992-93 data run, the initial store luminosity was typically 5×10^{30} cm^{-2}-sec^{-1}, five times the design luminosity of the Collider. The integrated luminosity recorded on tape was 19.3 (13.4) pb^{-1} for the CDF (D0) detectors.

Many results have been produced from these data. For example, 28 papers were submitted to the recent Rochester Conference by the CDF Collaboration. The time limitation prevents me from reporting on all the new CDF and D0 results. Instead, I present selected topics from the search for the top quark, tests of the Standard Model of electroweak interactions, studies of the strong interaction, the production and decay of states containing a b quark, and the search for new massive objects. Much of the material presented here is preliminary.

The CDF and D0 collaborations each have over 400 collaborators from the Americas, Europe, and Asia. The D0 detector, in its first data taking run, featured uranium liquid-argon calorimeters and a muon system with large rapidity coverage. CDF installed for this run a silicon vertex detector, which, when combined with precision tracking in the magnetic field, provided significant new physics capability.

2. Top Quark

If the Minimal Standard Model is correct, consistency of all electroweak data (Z decay, M_W, ν scattering, etc.) with the model requires[1]

$$M_{top}^{SM} = 177 \pm 11^{+18}_{-19}\ \mathrm{GeV/c^2}$$

An object this massive can only be produced at the Tevatron Collider. The dominant production mechanism is shown in Fig. 1. For an integrated luminosity of 20 pb^{-1},

Published Proceedings Eighth Meeting of the Division of Particles and Fields of the American Physical Society (DPF'94), University of New Mexico, Albuquerque, NM, August 2-6, 1994.

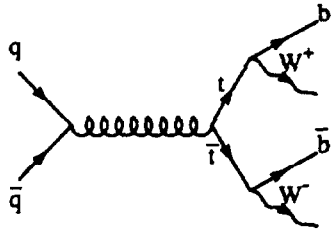

Fig. 1. The dominant top quark production mechanism in $\bar{p}p$ collisions.

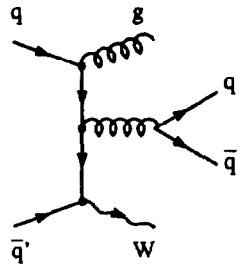

Fig. 2. The dominant background in the single lepton top search.

approximately 200 $t\bar{t}$ pairs should be produced. Decay branching ratios and detection efficiency reduces this to a small number of expected events.

Since both the top quark and W boson are very short lived, the experimental signature is determined by the decay of the two W bosons in each event. In order not to be overwhelmed by background, both CDF and D0 searched in two modes. The dilepton search seeks events in which both W's decay into $e\nu$ or $\mu\nu$ ($t\bar{t} \rightarrow ll\nu\nu b\bar{b}$). The product branching ratio is 5%. The single lepton search seeks events in which one W decays into $e\nu$ or $\mu\nu$ and the other decays into a light quark pair ($t\bar{t} \rightarrow l\nu q\bar{q}b\bar{b}$). Here the product branching ratio is 30%.

2.1. CDF Dilepton Search

The CDF top quark analysis was recently published.[2] In the dilepton mode, they search for ee, eμ, and $\mu\mu$ pairs of opposite electric charge. The minimum lepton P_T is 20 GeV/c, at least one of the leptons must be isolated, and ee and $\mu\mu$ pairs are removed if they are in the Z mass region - (75, 105) GeV/c^2. The missing E_T ($\not\!\!E_T$) must be at least 25 GeV, with the azimuthal angle between the missing E_T vector and the nearest jet or lepton required to be greater than 20° if $\not\!\!E_T$< 50 GeV. Finally, there must be at least 2 jets of E_T> 10 GeV and pseudorapidity $|\eta| < 2.4$.

The dominant backgrounds are WW production, Z→ $\tau\tau$, fake leptons, $b\bar{b}$ production, and lepton pairs coming from Drell-Yan production of γ^*/Z. The total background is $0.56^{+0.25}_{-0.13}$, compared to an expected signal of 1–2 events for a heavy top quark (140-180 GeV/c^2). CDF observes 2 events in this channel, as shown in Fig. 3.

2.2. CDF Single Lepton Search

The single lepton search begins with a selection of W→ $l\nu$ candidates: events containing an electron or muon with P_T> 20 GeV/c and $\not\!\!E_T$> 20 GeV. To suppress background without greatly reducing the top sensitivity, 3 or more jets with E_T> 15 GeV and $|\eta| < 2.0$ are required. There are 52 events in this sample. The dominant background is the production of a W recoiling against multiple jets (Fig. 2).

With these selection criteria, the expected signal to background ratio for a heavy top quark is approximately $\frac{1}{2}-\frac{1}{4}$. CDF further reduces the background by requiring that at least one of the b jets in the final state be identified. Two techniques are employed:

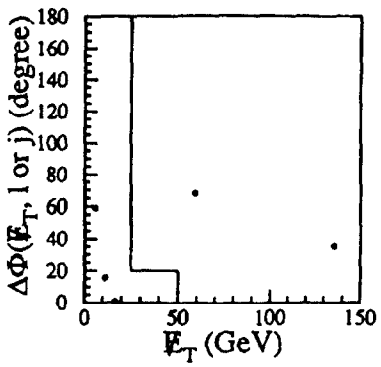

Fig. 3. The missing E_T vs. its angle relative to the nearest jet or lepton. The two events to the right of the cut line are top candidates.

finding the secondary vertex from the b decay, and finding an additional lepton from the semileptonic decay of the b or its daughter c quark.

For secondary vertex tagging, CDF uses jet data to determine the tagging efficiency and the background rate in high P_T jets. Figure 4 compares the proper decay distance ($c\tau$) distribution for b-tags in a b enriched sample of moderate P_T inclusive electron data with the prediction from a b Monte Carlo calculation. A similar distribution for data from a generic jet sample (Fig. 5) shows the contributions from false tags as well as the heavy quark content in such a sample. The efficiency for tagging at least one b jet in a $t\bar{t}$ event is $22 \pm 6\%$.

The dominant background comes from tagging errors plus the process shown in Fig. 2 in which the $q\bar{q}$ is a $b\bar{b}$ pair. The generic jet sample is used to measure the tag rate from these processes as a function of jet E_T and track multiplicity. This function is applied to each jet in the 52 event W + $\geq$ 3 jet sample to obtain the expected number of background tags. The total background is 2.30 ± 0.29 tags compared to 1.5–5 expected from heavy top. There are 6 tags observed in the data.

The second b tagging method searches for electrons or muons with $P_T > 2$ GeV/c, in order to be sensitive to leptons from both b decay and the decay of the daughter c quark. The efficiency for finding electrons is determined from a data sample of conversion electrons, while the muon efficiency is measured in $J/\psi \rightarrow \mu\mu$ data. The efficiency for tagging at least one b jet in a $t\bar{t}$ event is $16 \pm 2.5\%$. The dominant background is measured with generic jet events. The total background is 3.1 ± 0.3 tags, with 1–3.5 expected from a top quark signal. Seven tags are observed, 3 of which are in events that also have an identified secondary vertex. Figure 6 shows the total number of observed tags in W events as a function of the number of jets in the event. There is an excess over background in the top signal region ($\geq$ 3 jets).

2.3. CDF Top Search Summary

In total, CDF observes 15 counts (dilepton events, secondary vertex tags, soft lepton tags) in 12 events with $5.96^{+0.49}_{-0.44}$ counts expected from background. The probability that the background would fluctuate up to 15 counts is 0.26%, which is the 2.8

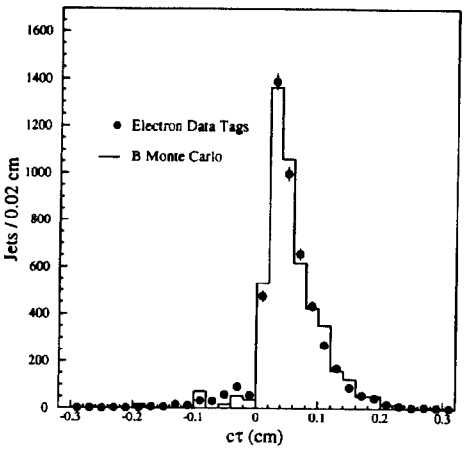

Fig. 4. The secondary vertex proper decay distance distribution from a b enriched sample of inclusive electrons compared to a Monte Carlo prediction.

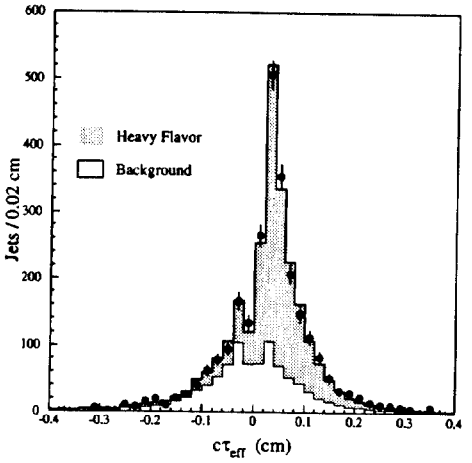

Fig. 5. The secondary vertex proper decay distance distribution from a sample of generic jet events. The contributions from tagging errors and heavy flavor jets are shown.

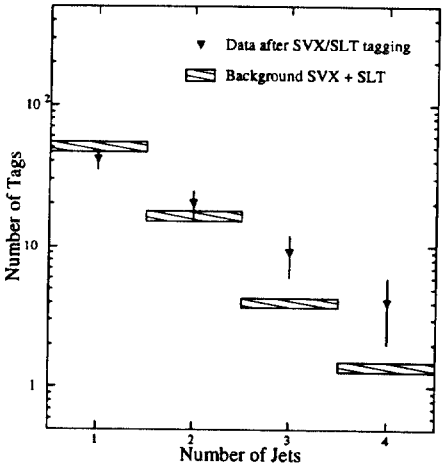

Fig. 6. The total number of observed b-tags (secondary vertex, SVX, and soft lepton, SLT) as a function of the number of jets in W events.

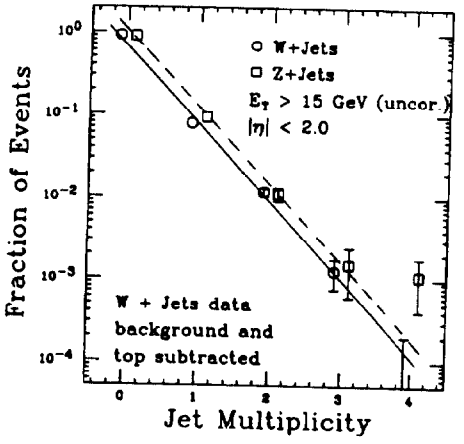

Fig. 7. The jet multiplicity distributions for Z events and for W events after subtracting the expected top quark and background contributions. The straight lines are to guide the eye.

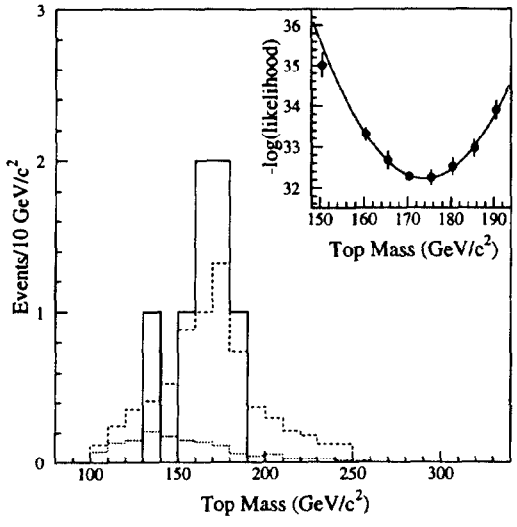

Fig. 8. The top quark mass from single lepton plus 4 jet events (solid), the expected background (dotted), and the expected shape for 175 GeV/c^2 top plus background (dashed). The insert shows the likelihood as a function of top mass.

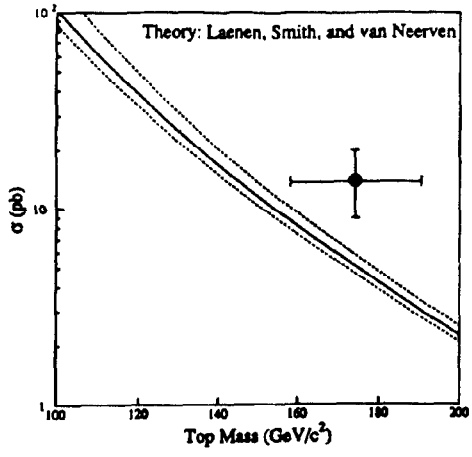

Fig. 9. The CDF measurement of the top quark mass and production cross section compared to a partial NNLO calculation.

σ point on a Gaussian distribution.

Single lepton events ($l\nu q\bar{q}b\bar{b}$) containing 4 jets can be reconstructed (2-C fit) to obtain the top quark mass. Of the 10 single lepton events with a b-tag, 7 have a fourth jet with $E_T > 8$ GeV. Figure 8 shows the mass from these 7 events along with the expected distribution from background and 175 GeV/c^2 top plus background. The best mass, extracted from a likelihood fit (see insert in Fig. 8), is

$$M_{top} = 174 \pm 10^{+13}_{-12}\ \text{GeV}/c^2.$$

The background subtracted number of events in each of the searches is used to calculate the $t\bar{t}$ production cross section, $\sigma = 13.9^{+6.1}_{-4.8}$ pb. Figure 9 compares the CDF mass and cross section with a partial next-to-next-to-leading-order calculation.[3]

There are additional features of the data that support the top hypothesis and others that do not. On the negative side, the estimated contributions from the top quark and other backgrounds account for all the observed W + $\geq$ 4 jet events, leaving little room for the dominant background (Fig. 2). Also in the control sample of Z + $\geq$ 3 jet events, there are two events with b-tags, compared to an expected 0.64 event.

Both of these effects can be seen in Fig. 7. It is clear that additional statistics will help a great deal.

On the positive side, one of the dilepton events has a jet containing both a secondary vertex and soft lepton tag. This is very unlikely to come from background sources that don't contain b-jets. In single lepton events, the kinematic distributions of the jets support the top hypothesis, and the mass fit prefers top plus background to background alone by a factor of 50 in relative likelihood.

2.4. D0 Dilepton Search

Early this year, the D0 collaboration published a lower top mass limit of 131 GeV/c^2 at the 95% CL.[4] At the end of April, they presented a status report on their analysis. Recently the analysis was updated, with slightly modified analysis cuts and recalculated backgrounds.

In the dilepton mode, D0 searches for eμ, ee, and $\mu\mu$ pairs. For the eμ case, the electron (muon) transverse momentum must be greater than 15 (12) GeV/c. The missing E_T in the calorimeter must be greater than 20 GeV, and after correcting for the muon momentum it must be greater than 10 GeV. In the ee case, both electrons must have $P_T > 20$ GeV/c, and the missing E_T must be greater than 25 GeV. For muon pairs, the muon P_T must be greater than 15 GeV/c and the azimuthal angle between the muons must be less than 140° if $\not\!\!E_T < 40$ GeV. Finally, all dilepton events must have at least 2 jets with $E_T > 15$ GeV.

The total estimated background in the dilepton mode is $0.76 \pm \sim 0.15$ events.* For a heavy top quark, 0.5–1.5 events are expected. D0 observes 1 dilepton event.

2.5. D0 Single Lepton Search

For the single lepton mode, D0 separately considers events with and without a b-tag. Their b-tagging algorithm is applied in electron plus jet events and requires an additional muon of $P_T > 4$ GeV/c.

In the single lepton search without b-tagging, D0 requires either an electron with $P_T > 20$ GeV/c or a muon with $P_T > 15$ GeV/c. $\not\!\!E_T$ must be greater than 25 GeV for electron events, while for muon events both the calorimeter $\not\!\!E_T$ and the muon corrected $\not\!\!E_T$ must be greater than 20 GeV. To suppress background, three event topology requirements are made. There must be at least 4 jets of $E_T > 15$ GeV and $|\eta| < 2$, the aplanarity of the event must be greater than 0.05, and the event transverse energy variable, H_T, must be above 140 GeV. In electron events, H_T is the scalar sum of the transverse energies of the jets and the W. For muon events, only the jets are included.

The total background is $1.8 \pm \sim 1$ events, compared to 1.5–4 expected from a heavy top quark. D0 observes 4 events in this mode.

The D0 b-tag search includes events with an electron of $P_T > 20$ GeV/c, missing E_T in the calorimeter greater than 20 GeV, 3 jets with $E_T > 20$ GeV and $|\eta| < 2$, and a muon with $P_T > 4$ GeV/c. The contribution of b decay in a low P_T inclusive muon data sample can be seen in Fig. 10, which shows the P_T of the muon relative to the nearest jet.

---

*The quoted uncertainties in the dilepton and single lepton without b-tag modes are my estimates, since I have combined a few of their search modes. In the D0 top search summary, however, the total background and its uncertainty are as quoted by D0.

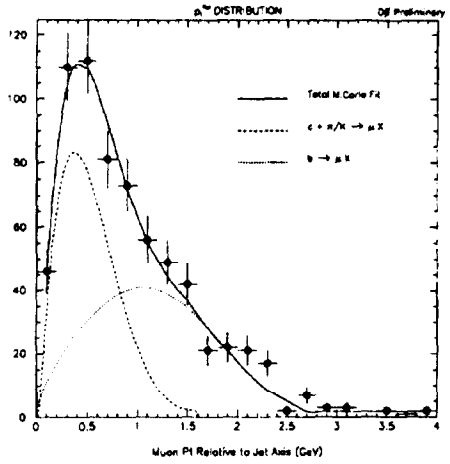

Fig. 10. The transverse momentum of the muon relative to the nearest jet axis. The D0 data are compared to a fit (solid) to the sum of two shapes: b-decay (dotted), and charm/π/K decay (dashed).

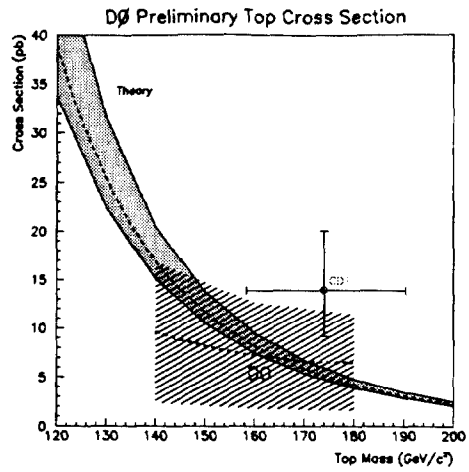

Fig. 11. The D0 top quark production cross section compared with theory and the CDF result. The D0 cross section varies slightly with top mass because the efficiency of the event selection criteria depends on the mass.

The total background in this mode is 0.55 ± 0.15 events. Between 0.5 and 1.5 events are expected from a heavy top quark. D0 observes 2 events.

2.6. D0 Top Search Summary

The total background for all the D0 modes is 3.2 ± 1.1 events, while 2.5-6.5 events are expected for a top quark of mass between 140 and 180 GeV/c^2. D0 observes 7 events. As seen in Fig. 11, the D0 result is consistent with either the no-top hypothesis or the CDF result.

2.7. Top Prospects

In the current Tevatron Collider run, each experiment should accumulate approximately four times the data they acquired in the 1992-93 run. That should not only allow for confirmation of the CDF result, but also provide a top mass measurement with an uncertainty of 8-10 GeV/c^2.

The Fermilab Main Injector is now under construction. By the end of the decade, there should be 500–1000 top events between the two experiments. With this quantity of data, the mass uncertainty could drop to 5 GeV/c^2. A sensitive search for non-standard decay modes of the top quark will be under way, and the systematic study of top quark couplings will have begun.

3. W Mass

Precision measurements of Z^0 decay provide a prediction of the W mass to approximately ± 100 MeV/c^2, assuming that the Minimal Standard Model is correct.[1]

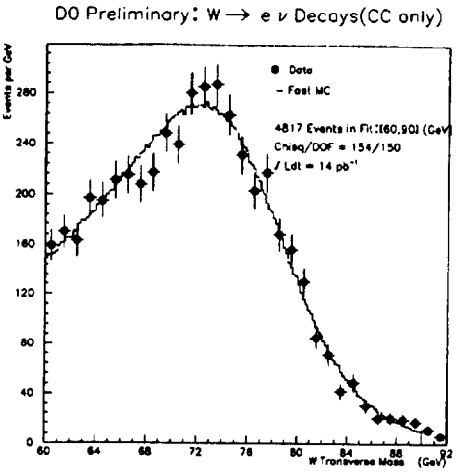

Fig. 12. The D0 W→ $e\nu$ transverse mass plot. The histogram is the best fit Monte Carlo line shape.

Since the W production cross section is approximately 20 nb at the Tevatron, there are thousands of leptonic W decay events (W→ $l\nu$) in each experiment even after applying the tight fiducial cuts needed for a precision mass measurement. The $l\nu$ invariant mass cannot be calculated because of the undetected neutrino. Instead the two dimensional analog, transverse mass, is used, with the neutrino transverse momentum taken as balancing the visible transverse momentum in the event.

$$\begin{aligned} M_T^W &= \sqrt{2P_T^l P_T^\nu (1 - cos\,\phi_{l,\nu})} \\ \vec{P}_T^{\,\nu} &= -\vec{P}_T^{\,l} - \vec{P}_T^{\,\text{hadrons}} \end{aligned}$$

The D0 measurement uses 5830 W→ $e\nu$ events. CDF has 6421 W→ $e\nu$ and 4090 W→ $\mu\nu$ events. Figure 12 shows the transverse mass distribution from D0, while Fig. 13 and Fig. 14 show the CDF distributions.

The critical issues for the measurement, as seen in the equations above, are the lepton energy scale and resolution, and the response of the detector to the hadron system recoiling against the W. Much of the needed information comes from $Z^0 \rightarrow l^+l^-$ events.

Both groups obtain the lepton energy resolution from test beam studies and the measured $Z^0 \rightarrow l^+l^-$ line shape. D0 obtains its absolute electron energy scale from the reconstructed Z mass (Fig. 15). Although their absolute scale is low by 4%, the W mass is close enough to the Z mass that they can rescale without incurring a very large systematic uncertainty. The CDF energy scale is determined in two steps. First the calorimeter electron scale is tied to the magnetic spectrometer using the ratio of the calorimeter energy to the tracking chamber momentum (Fig. 16). Second, the absolute scale of the spectrometer is checked with the J/ψ, Υ, and Z^0 masses (Fig. 17 and Fig. 18).

Modeling the response of the calorimeters to the recoil hadron system is handled

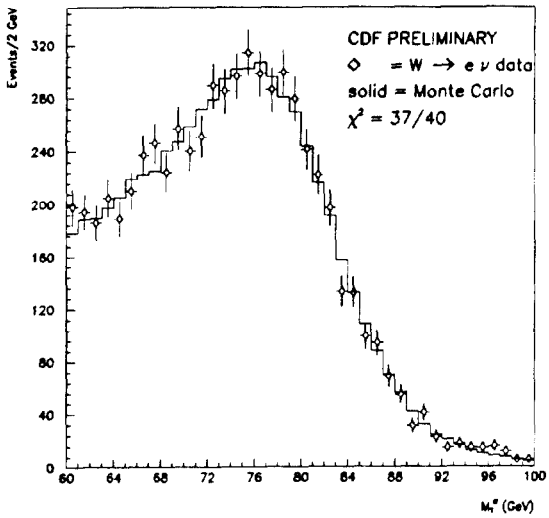

Fig. 13. The CDF W→ $e\nu$ transverse mass plot. The histogram is the best fit Monte Carlo line shape.

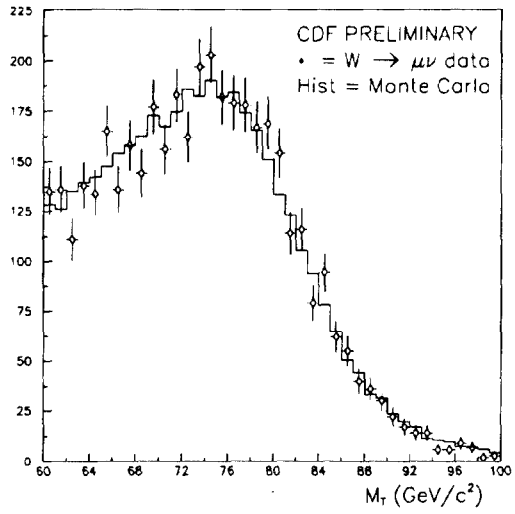

Fig. 14. The CDF W→ $\mu\nu$ transverse mass plot. The histogram is the best fit Monte Carlo line shape.

differently in the two experiments. In the D0 Monte Carlo, the W recoil system is treated as a single jet, with the D0 jet energy resolution applied and the scale determined from Z^0 events (Fig. 19). CDF notes that the detector response to the hadrons recoiling against a vector boson of $\vec{P}_T^V$ is the same whether the boson is a W or a Z^0. Thus for each Monte Carlo W, the rest of the event is taken from a Z^0 **data** event of the same P_T (Fig. 20).

Both CDF and D0 obtain the W mass by fitting Monte Carlo templates to the W→ $l\nu$ transverse mass distributions (Fig. 12, Fig. 13, Fig. 14). The systematic uncertainties are given in Fig. 21 and Fig. 22. All of them can be studied with the data. Even the structure function uncertainty (from the u to d quark ratio) can be directly measured with the CDF W asymmetry data (Fig. 23).

The masses obtained by the two collaborations are:

$$\begin{aligned} \text{D0}: \quad M_W = \; & 79.86 \pm 0.16 \pm 0.16 \pm 0.26(\text{scale}) \text{ GeV}/c^2 \\ & 79.86 \pm 0.345 \text{ GeV}/c^2 \end{aligned}$$

$$\begin{aligned} \text{CDF}: \quad & 80.47 \pm 0.15 \pm 0.25 \text{ GeV}/c^2 \;\; (W \to e\nu) \\ & 80.29 \pm 0.20 \pm 0.24 \text{ GeV}/c^2 \;\; (W \to \mu\nu) \\ & 80.38 \pm 0.23 \text{ GeV}/c^2 \;\; (\text{CDF combined}) \end{aligned}$$

The new world average, combining these results with earlier results from CDF[5] and

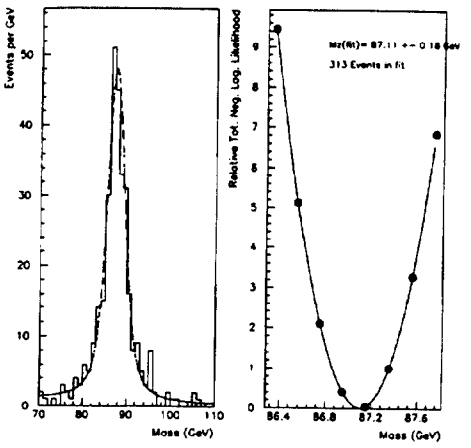

Fig. 15. The D0 Z→ ee mass peak with the fit line shape and the negative log-likelihood plot used to determine the mass.

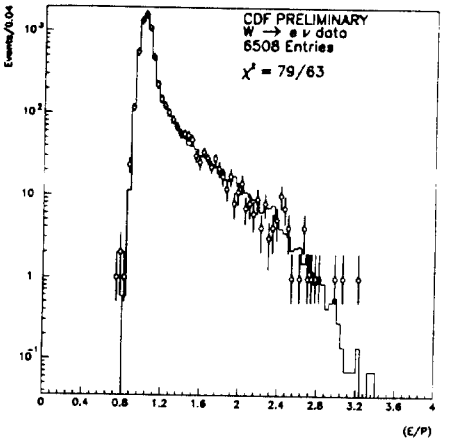

Fig. 16. The ratio of calorimeter energy to tracking chamber momentum in CDF W→ $e\nu$ electrons compared to the prediction of a radiative W Monte Carlo. The high side tail is due to electron bremsstrahlung.

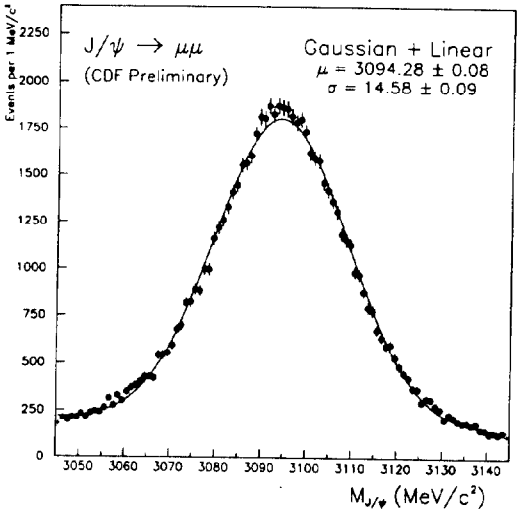

Fig. 17. The CDF J/ψ → $\mu\mu$ mass peak.

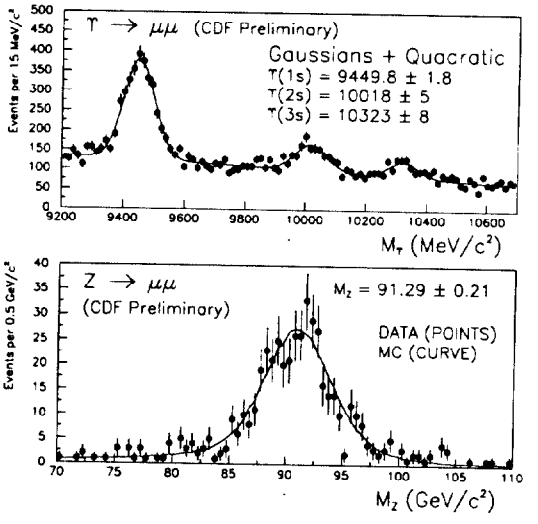

Fig. 18. The Υ resonances and the Z peak from CDF.

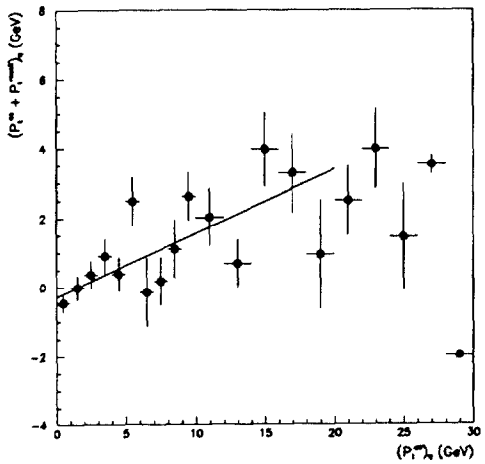

Fig. 19. The sum of the $\vec{P}_T$ of the recoil hadrons and the two electrons in D0 Z→ *ee* events as a function of the P_T of the electron pair. Plotted is the component of these vectors along the bisector of the two electron directions.

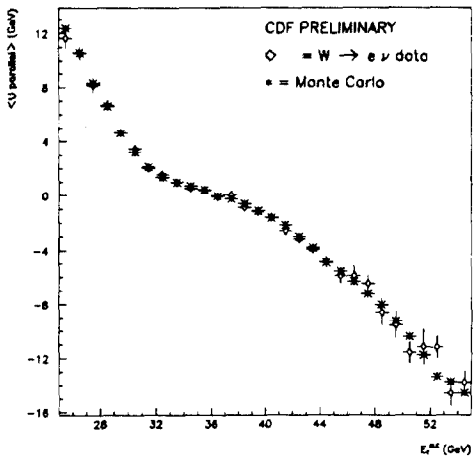

Fig. 20. The component of the net recoil hadron transverse momentum along the electron direction in CDF W→ *eν* events as a function of the electron E_T.

Source of Uncertainty	MeV/c^2
Trigger Efficiency	20
Resolution and neutrino E_T scale	149
Energy underlying electron	50
$U_{//}$ efficiency	10
Hadronic to EM scale	80
QCD background	30
Theoretical model uncertainty	86
W width	20
Fitting Error	30
Total	200

Resolution and neutrino E_T scale	
Electron energy resolution	70
Neutrino E_T scale, resolution (W underlying event)	130
Jet energy resolution	20

Theoretical model uncertainty	
Structure function	70
P_{tw} spectrum	50

Fig. 21. The D0 W mass systematic uncertainties.

	$W \to e\nu$	$W \to \mu\nu$	Correlated	Uncorrelated	
				$W \to e\nu$	$W \to \mu\nu$
Statistical	150	200		150	200
Momentum Scale	130	60	60	120	
Systematics	210	220			
Momentum Resolution	140	120		140	120
P_T^W	90	110	80	40	70
$u_{\|\|}$	70	90		70	90
Backgrounds	50	50		50	50
Fitting	20	20		20	20
Structure Functions	100	100	100		
Total	290	300	140	260	270

Fig. 22. The CDF W mass uncertainties.

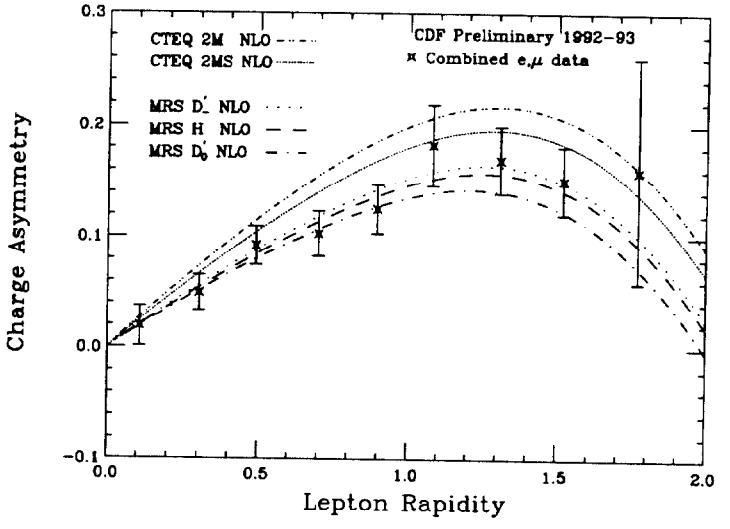

Fig. 23. The CDF lepton charge asymmetry in W decay compared to several modern structure functions.

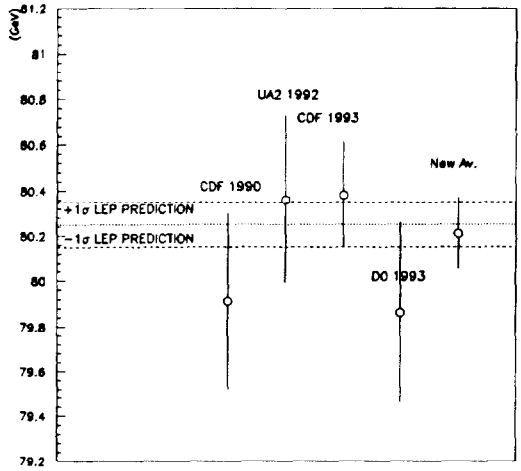

Fig. 24. The experimental measurements of the W mass.

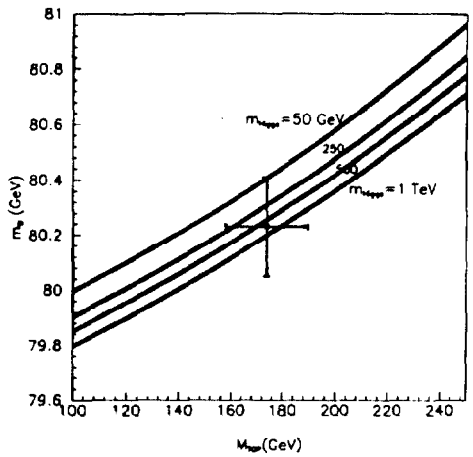

Fig. 25. The W and top quark mass measurements compared to the predictions of the Minimal Standard Model for different Higgs boson masses.

UA2,[6] is (Fig. 24)

$$80.23 \pm 0.18 \text{ GeV}/c^2 \text{ (CDF, D0, UA2)}$$

We now have the first experimental point on the M_W vs. M_{top} plot (Fig. 25). Since the systematics of the M_W measurement are statistics limited (Z^0 events, W asymmetry data), the uncertainty should continue to be reduced with increasing integrated luminosity. It seems quite possible that ± 50 MeV/c^2 could be reached by the end of the decade. When combined with a top quark mass measurement of ± 5 GeV/c^2, we would have a data point on Fig. 25 that would severely test the Minimal Standard Model. If the model is correct, then the data could discriminate between a light and a heavy Higgs boson.

4. Vector Boson Pair Production

In the Standard Model, the triboson couplings are specified. In some non-standard models, the vector bosons are composite, resulting in anomalous triboson couplings which modify the electric and magnetic multipole moments of the bosons. These can be determined by looking at the production rate and kinematic properties of boson pairs ($W\gamma$, $Z\gamma$, WW, WZ, ZZ) produced in $\bar{p}p$ collisions.

As an example, I consider $W\gamma$ production. If CP conservation is assumed, there are two anomalous couplings, usually written as $\Delta\kappa$ and λ. The magnetic dipole and electric quadrupole moments of the W are related to these couplings:

$$\mu_W = \frac{e}{2M_W}(2 + \Delta\kappa + \lambda)$$

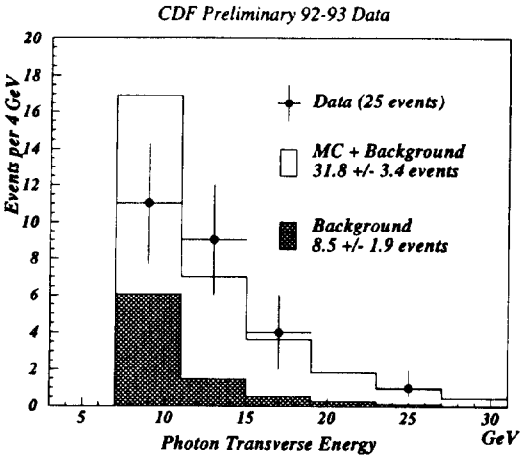

Fig. 26. The photon P_T in CDF W events compared to the calculated background and the expected signal from Standard Model couplings.

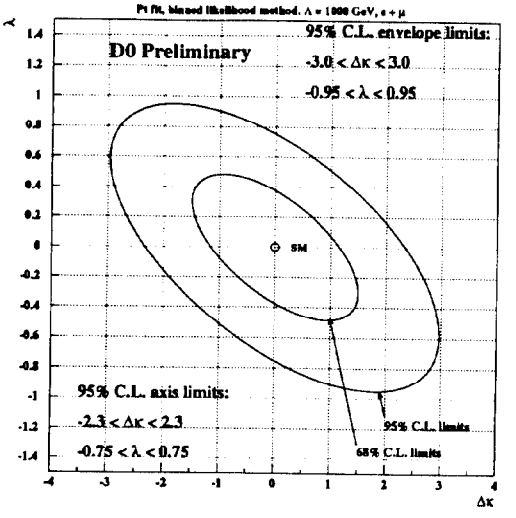

Fig. 27. The D0 limit on the anomalous couplings $\Delta\kappa$ and λ from Wγ data.

$$Q_W^e = \frac{-e}{M_W^2}(1 + \Delta\kappa - \lambda)$$

CDF and D0 have searched for high P_T photons in W events. In D0 the minimum E_T is 10 GeV, while in CDF it is 7 GeV. In both experiments, the photon is required to be at least a distance 0.7 (in $\eta - \phi$ space) away from the charged lepton in order to suppress the contribution from e/μ bremsstrahlung. CDF (D0) finds 25 (19) events, which after background subtraction becomes 16.5 (13.8). The photon P_T distribution is shown in Fig. 26. The shape of the distribution is used to extract the anomalous couplings. Figure 27 shows the D0 contours for $\Delta\kappa$ and λ. The CDF limits are very similar. Limits for CP violating anomalous WWγ couplings as well as CP conserving and violating ZZγ anomalous couplings have also been extracted by the two experiments.

5. Inclusive Photon Production

Inclusive photon production in high energy $\bar{p}p$ collisions is a simple process at leading order ($qg \rightarrow \gamma q$) with a well defined and measured final state parton. The cross section can be used to determine the gluon distribution function in the proton. In addition, events with a final state photon and charm quark (through its daughter e or μ) provide a measure of the charm content of the proton.

The major experimental background comes from jets that fragment largely into a π^0 or η, which decay into photon pairs. CDF uses two methods to separate single

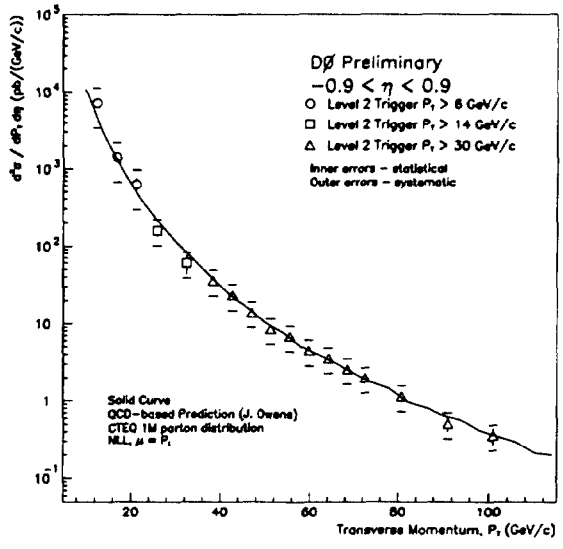

Fig. 28. D0 inclusive photon cross section as a function of the γ P_T compared with a theoretical prediction.

photons from the multiple photon background. In the profile method, they use the transverse shower shape approximately six radiation lengths into the shower to differentiate a single photon narrow shower from the broader shower induced by multiple photons. In the conversion method, they use the fraction of γ candidates that convert in the one radiation length solenoid coil. That fraction depends on whether one or multiple photons passed through the coil. For both methods, they measure the efficiency and separation power using reconstructed wide angle $\eta \rightarrow \gamma\gamma$ and $\rho^{\pm} \rightarrow \pi^0\pi^{\pm}$ events. The D0 group counts the number of candidates that convert in their tracking chamber.

The D0 data (Fig. 28) agree well with the predicted cross section. The CDF results have significantly smaller uncertainties. Although qualitatively they agree with next-to-leading-order QCD[7] (Fig. 29), when the comparison is made on a linear scale (Fig. 30) the agreement is not so good. At high P_T, there is no problem; however at low P_T the slope of the data is at variance with the theory. There are several possible explanations for the disagreement. The contribution from gluon-charm scattering may not be correct. The bremsstrahlung diagrams, where a photon is radiated from an initial state or final state parton, first appear in next-to-leading-order. There thus may be important NNLO contributions. Another possibility is that the assumed gluon distribution is not correct. A light gluino (1–5 GeV/c^2) could affect the cross section. Finally, the calculated K_T smearing (the effective initial state parton transverse momentum) may be too small. At the quantitative level, the last possibility may well have the largest effect. K_T smearing with a sigma that increases from 1 GeV/c at ISR energy to about 3 GeV/c at Tevatron energies improves the agreement between theory and the ISR, S$\bar{p}$pS, and Tevatron data.

6. b Production Cross Section

Studying the b production cross section is interesting because, at Tevatron energies, higher order QCD diagrams (ex, $gg \rightarrow gg \rightarrow gb\bar{b}$) can dominate over the leading order diagrams (ex, $gg \rightarrow b\bar{b}$). Also, as we shall see, it has led us to reexamine the dominant mechanisms for producing charmonium states.

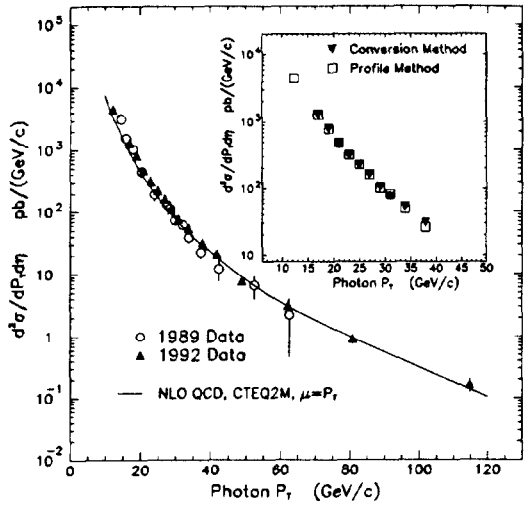

Fig. 29. CDF inclusive photon cross section compared to a QCD prediction.

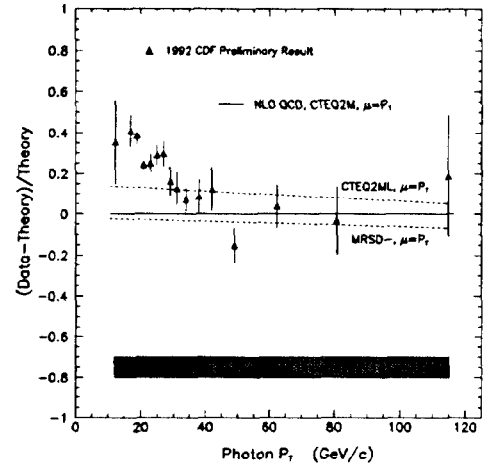

Fig. 30. The difference between the CDF inclusive photon cross section and theory as a fraction of the theoretical prediction.

D0 has measured single muon and dimuon production rates. Figure 31 shows their muon production cross section as a function of muon P_T. It is compared with the sum of the dominant sources of muons: b decay, c decay, π/K decay, and W decay. They extract the b production cross section using the ISAJET prediction of the fraction of muons coming from b decay. This prediction is checked in the data by looking at the P_T of the muon relative to the nearest jet (Fig. 10).

CDF measures the b production cross section by studying inclusive e, μ, J/ψ, and ψ', the semi-exclusive modes eD, μD, and μD^*, as well as the exclusive final states $J/\psi\, K$ and $J/\psi\, K^*$. Figure 32 shows the right sign and wrong sign μDπ combinations. The ψ and ψ' mass peaks are shown in Fig. 33 and Fig. 34.

There has been a significant change since results were presented by CDF in 1990, namely the b production cross section deduced from the inclusive J/ψ and ψ' rates have gone down by a factor of 2–3, even though the inclusive J/ψ and ψ' cross sections have not changed. In 1990, theoretical guidance was used to go from the charmonium cross section to the b cross section. It was believed that there are two important sources of J/ψ: B decay and χ_c decay. Because the χ mass is below that of the ψ', it was expected that the only significant source of ψ' would be B decay.

The installation of the silicon vertex detector for the 1992-93 run made it possible to separate prompt production from B decay. Figure 35 shows the proper decay length distribution for the ψ' sample. After background subtraction, it is found that only $22.8 \pm 3.5\%$ of the ψ' comes from B decay, compared to the expected $\sim$ 100%. Figure 36

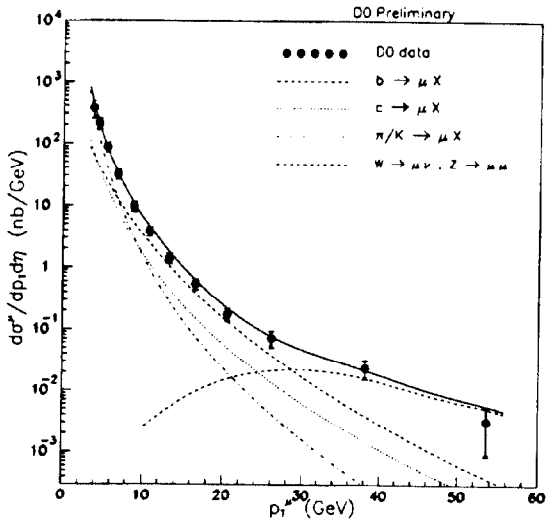

Fig. 31. D0 inclusive muon cross section as a function of the muon P_T. Also shown are the expected contributions from b decay, c decay, π/K decay, and W decay.

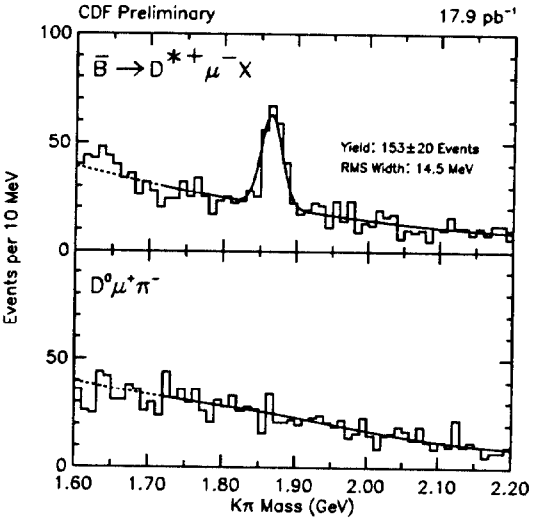

Fig. 32. The Kπ mass distribution in right sign and wrong sign μK$\pi\pi$ events. The D peak is seen for the charge combination allowed in B decay.

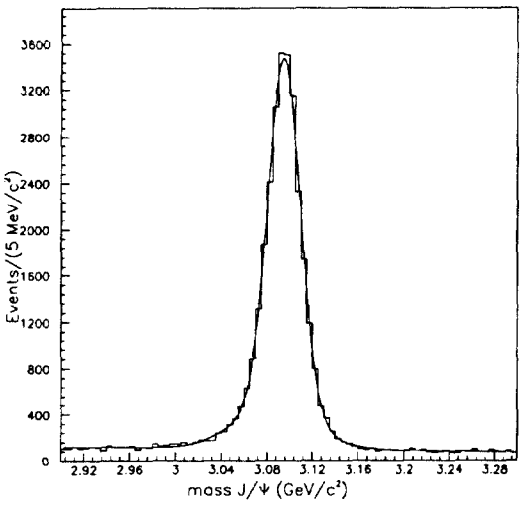

Fig. 33. The $\mu^+\mu^-$ mass distribution in the J/ψ region.

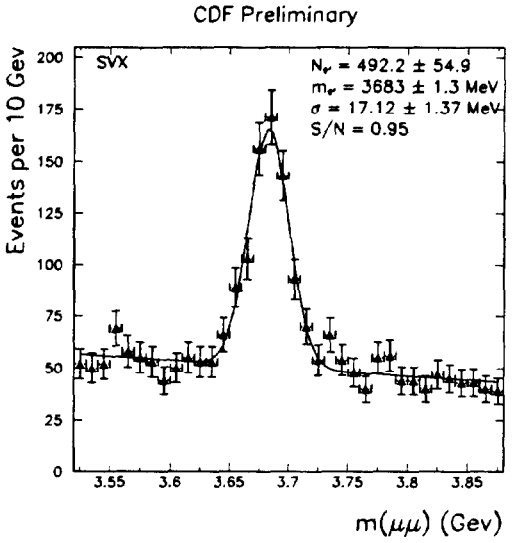

Fig. 34. The $\mu^+\mu^-$ mass distribution in the ψ' region.

shows the direct and B decay contributions to the ψ' cross section. The B component is in the range predicted by theory. The direct component, however, is much larger than predicted.[8]

A number of theorists are working on this problem.[8-10] Higher order fragmentation of a gluon or c quark into charmonium seems to be important. Figure 37 and Fig. 38 compare the CDF direct charmonium data with the leading order calculation as well as with the addition of fragmentation.[8] In the case of the J/ψ, the new calculation is close to the data. For the ψ', however, the calculated cross section is still much too small. There is clearly much to be done by the theorists to understand these discrepancies. The experimenters also have some issues to resolve, for example the difference between the CDF and D0 b cross sections at $P_T < 10$ GeV/c (Fig. 39). These issues will be easier to study now that sufficiently high statistics data are available to produce true differential cross sections (Fig. 40).

7. B Lifetimes

For many of the important B physics goals of the future, a large production cross section is not sufficient. It has to be shown that precision measurements can be made with the B mesons. To show that this can be done in a high luminosity hadron collider environment, I want to briefly present recent work measuring the B meson lifetimes.

CDF has published measurements of the average B lifetime[11] and the lifetimes for the charged and neutral B mesons using fully reconstructed decays.[12] Figure 41 shows the proper decay length distribution used to obtain the average B lifetime.

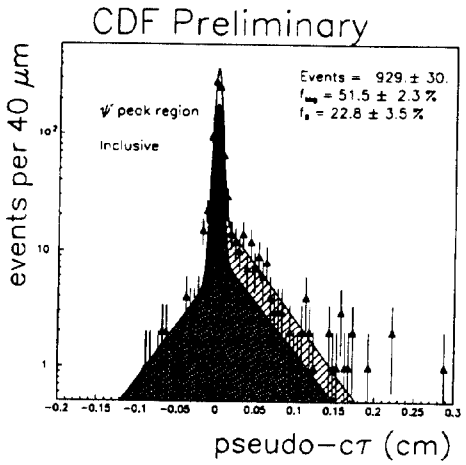

Fig. 35. The lifetime distribution from ψ''s. The dark cross-hatched area is the background obtained from the mass sidebands.

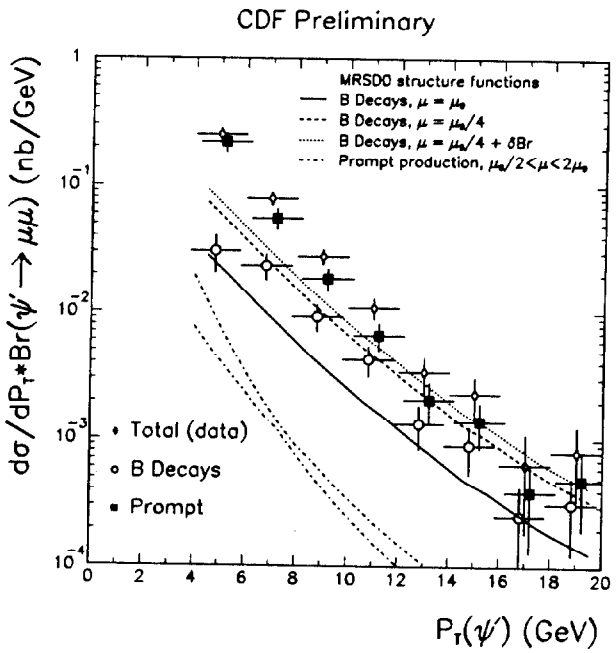

Fig. 36. The differential cross section for producing ψ' separated into the prompt and B decay contributions and compared with theoretical predictions.

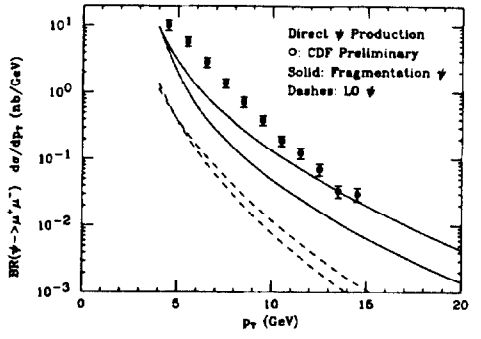

Fig. 37. The comparison made by Braaten *et al.* of CDF data with the leading order and fragmentation contributions to direct J/ψ production.

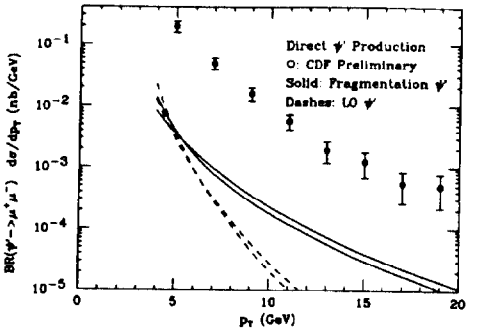

Fig. 38. The comparison made by Braaten *et al.* of CDF data with the leading order and fragmentation contributions to direct ψ' production.

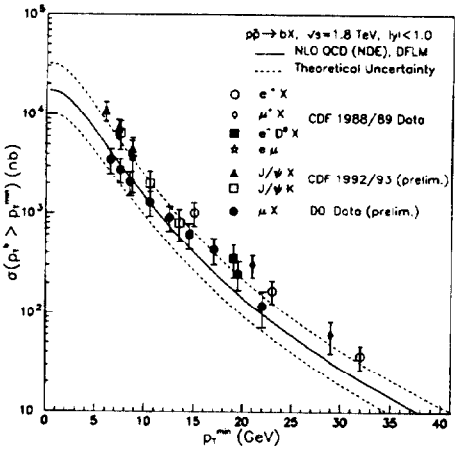

Fig. 39. The D0 and CDF b cross section as a function of P_T. Each point represents the integrated cross section above that P_T.

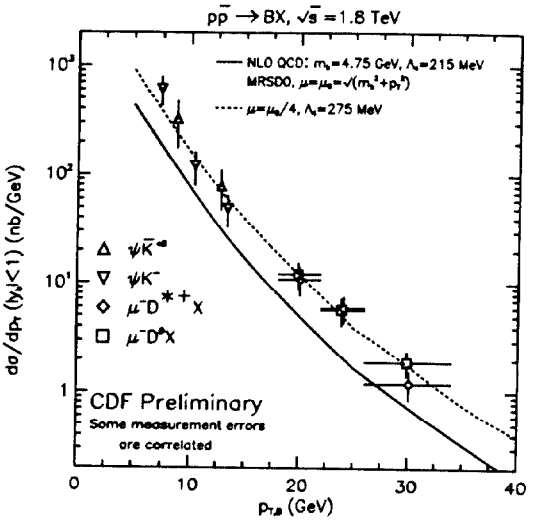

Fig. 40. The differential b production cross section measured by CDF.

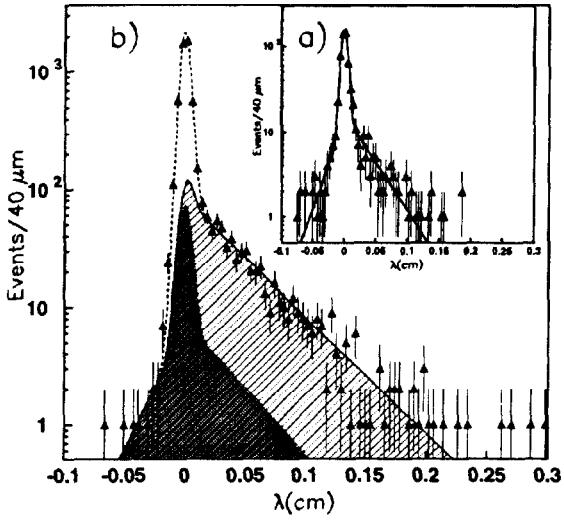

Fig. 41. The CDF B proper lifetime from inclusive J/ψ's.

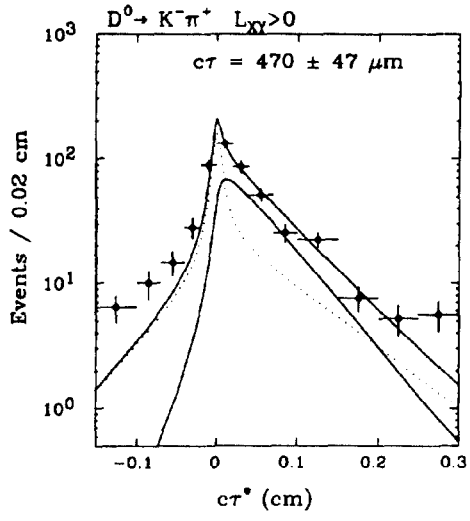

Fig. 42. The B lifetime from CDF eD^0 events. The inner solid line is the signal contribution, while the outer solid line is the signal plus the background as determined from the mass sidebands (dotted).

Recently CDF has included the semi-exclusive eD and eD* final states to help measure the individual B meson lifetimes (Fig. 42). The values obtained for the B^- are:

$$e^-D^0X \quad \tau_- = 1.52 \pm 0.21^{+0.09}_{-0.10} \text{ psec}$$
$$J/\psi\, K^- \quad \tau_- = 1.61 \pm 0.16 \pm 0.05 \text{ psec}$$

For the $\overline{B}^0$, the results are:

$$e^-D^{*+}X \quad \tau_0 = 1.63 \pm 0.16 \pm 0.09 \text{ psec}$$
$$J/\psi\, K^{*0} \quad \tau_0 = 1.57 \pm 0.18 \pm 0.08 \text{ psec}$$

The resulting ratio of the charged to neutral B lifetime is

$$\frac{\tau(B^-)}{\tau(\overline{B}^0)} = 0.98 \pm 0.13$$

Figure 43 shows this measurement compared to those at LEP.

CDF has also measured the lifetime of the B_s meson using both exclusive and semi-exclusive (Fig. 44) final states. The results below are compared with other measurements in Fig. 45.

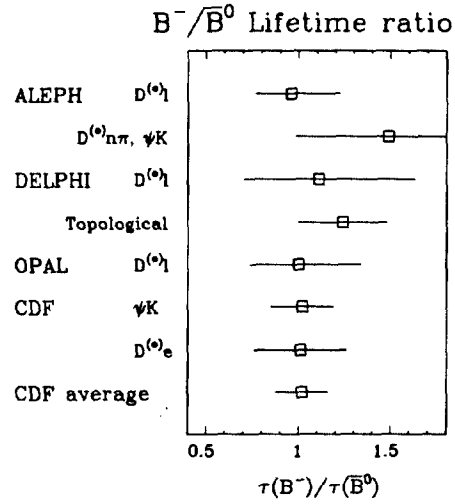

Fig. 43. The charged to neutral B lifetime ratio.

$e/\mu^- D_s^+$ $\quad \tau_s = 1.42^{+0.27}_{-0.23} \pm 0.11$ psec
$J/\psi\,\phi$ $\quad \tau_s = 1.74^{+0.90}_{-0.60} \pm 0.07$ psec

8. Searching for New Heavy Objects

The Fermilab Tevatron Collider is at the "energy frontier" and should remain there for the next decade. It is thus important to search for new massive objects. Because of a lack of time, I will only present the current limits, all at the 95% CL.

Both CDF and D0 have new limits for heavy vector bosons. Assuming standard couplings, CDF (D0) find that the mass of a W′ must be greater than 652 (620) GeV/c^2, while a Z′ must have a mass greater than 505 (480) GeV/c^2.

D0 has a new limit on first generation leptoquarks.[13] If its spin is 0 and its branching ratio into eq is 1, the mass must be greater than 130 GeV/c^2 (Fig. 46). The mass limit for a spin 1 leptoquark is a factor of 1.5–2 higher. CDF has searched for second generation leptoquarks and finds that if BR(LQ$\rightarrow \mu q$)=1.0, the mass must be greater than 133 GeV/c^2 (Fig. 47).

D0 has a new limit on gluinos. They select the Minimal Supersymmetric Standard Model parameters $\tan\beta = 2$, $\mu = -250$ GeV, and $m_{H^+} = 500$ GeV. They find that the gluino mass must be $>$ 146 GeV/c^2 @ 90% CL for very large squark mass, and it must be $>$ 205 GeV/c^2 @ 90% CL for equal squark and gluino masses.

Finally, CDF has a set of limits for particles that decay into jet pairs. They exclude axigluons in the range 200<M<920 GeV/c^2, a color octet technirho[14] in the range 260<M<470 GeV/c^2 if the branching ratio of the technirho into dijets is 1,

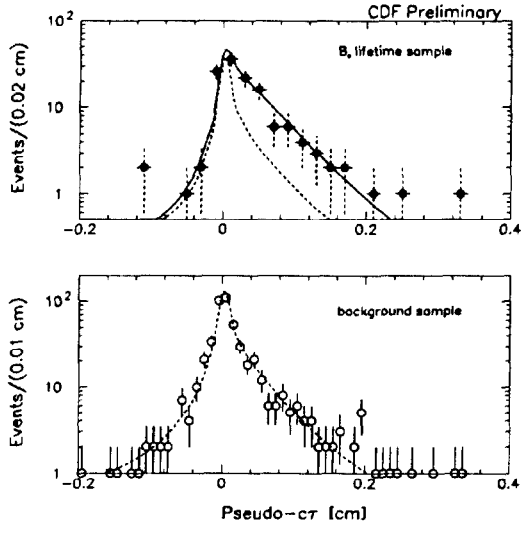

Fig. 44. The B_s lifetime from CDF lD_s events.

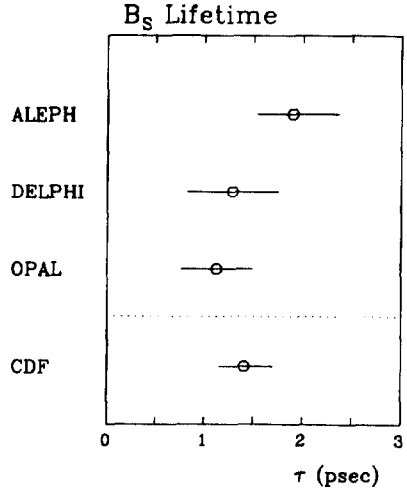

Fig. 45. B_s lifetime measurements.

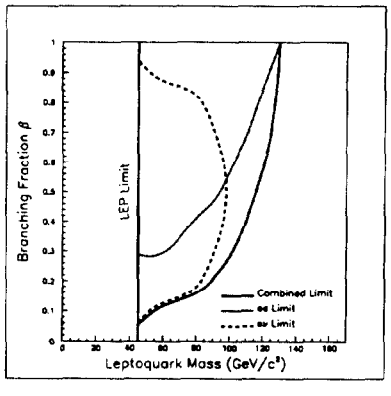

Fig. 46. The D0 1st generation leptoquark mass limit as a function of its branching ratio into eq

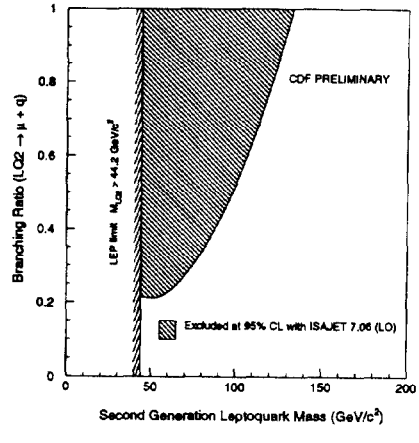

Fig. 47. The CDF 2nd generation leptoquark mass limit as a function of its branching ratio into μq

and excited quarks with mass below 620 GeV/c^2 if they have standard couplings. The excited quark search looks at three modes: $q^* \rightarrow qW$ and $q^* \rightarrow q\gamma$ in addition to the dijet mode ($q^* \rightarrow qg$).

9. Conclusions

The most exciting result of the past year is the evidence for the top quark. At a mass of 174 GeV/c^2, the top quark Yukawa coupling is 1. This makes the top quark a potentially powerful laboratory for learning about mass generation.

There were many other analyses in the past year that addressed important issues in electroweak interactions, QCD, b physics, and the search for new massive objects. Hopefully, much more information will be forthcoming in all of these areas with the data from the current Tevatron Collider run, which should increase the existing data sample by a factor of 4.

References

1. B. Pietrzyk, *Proceedings of the XXIXth Rencontres de Moriond* (1994).
2. F. Abe *et al.*, *Phys. Rev. Lett.* **73** (1994) 225. The details of this analysis are presented in F. Abe *et al.*, *Phys. Rev.* **D50** (Sept. 1, 1994).
3. E. Laenen *et al.*, *Phys. Lett.* **B321** (1994) 254.
4. S. Abachi *et al.*, *Phys. Rev. Lett.* **72** (1994) 2138.
5. F. Abe *et al.*, *Phys. Rev. Lett.* **65** (1990) 2243.
6. J. Alitti *et al.*, *Phys. Lett.* **B276** (1992) 354. The W mass is calculated using 91.187 $\pm$ 0.007 GeV/c^2 for the Z mass.
7. J. Ohnemus *et al.*, *Phys. Rev.* **D42** (1990) 61.
8. E. Braaten *et al.*, FERMILAB-PUB-94/135-T (1994).
9. M. Cacciari and M. Greco, FNT/T-94/13 (1994).
10. D.P. Roy and K. Sridhar, CERN-TH.7329/94 (1994).
11. F. Abe *et al.*, *Phys. Rev. Lett.* **71** (1993) 3421.
12. F. Abe *et al.*, *Phys. Rev. Lett.* **72** (1994) 3456.
13. S. Abachi *et al.*, *Phys. Rev. Lett.* **72** (1994) 965.
14. K. Lane and M. Ramana, *Phys. Rev.* **D44** (1991) 2678; E. Eichten and K. Lane, *Phys. Lett.* **B327** (1994) 129.